Matrilin-3 Is Dispensable for Mouse Skeletal Growth and Development

Yaping Ko,[1] Birgit Kobbe,[1]† Claudia Nicolae,[2]† Nicolai Miosge,[3]
Mats Paulsson,[1] Raimund Wagener,[1] and Attila Aszódi[2]*

Center for Biochemistry, Medical Faculty, University of Cologne, D-50931 Cologne,[1] Center of Anatomy, Department of Histology, University of Göttingen, D-37075 Göttingen,[3] and Department for Molecular Medicine, Max Planck Institute for Biochemistry, D-82152 Martinsried,[2] Germany

Matrilin-3 belongs to the matrilin family of extracellular matrix (ECM) proteins and is primarily expressed in cartilage. Mutations in the gene encoding human matrilin-3 (*MATN-3*) lead to autosomal dominant skeletal disorders, such as multiple epiphyseal dysplasia (MED), which is characterized by short stature and early-onset osteoarthritis, and bilateral hereditary microepiphyseal dysplasia, a variant form of MED characterized by pain in the hip and knee joints. To assess the function of matrilin-3 during skeletal development, we have generated *Matn-3* null mice. Homozygous mutant mice appear normal, are fertile, and show no obvious skeletal malformations. Histological and ultrastructural analyses reveal endochondral bone formation indistinguishable from that of wild-type animals. Northern blot, immunohistochemical, and biochemical analyses indicated no compensatory upregulation of any other member of the matrilin family. Altogether, our findings suggest functional redundancy among matrilins and demonstrate that the phenotypes of MED disorders are not caused by the absence of matrilin-3 in cartilage ECM.

Matrilin-3 is a member of the matrilin family of extracellular matrix proteins characterized by a modular structure made up of von Willebrand factor A (vWFA) domain(s), epidermal growth factor (EGF)-like domain(s), and a coiled-coil α-helical oligomerization domain (for a review, see reference 10). The genomes of human and mouse contain four matrilin genes, which are differentially expressed. Matrilin-1 and matrilin-3 are mainly present in skeletal tissues (1, 16), whereas matrilin-2 and matrilin-4 (17, 23, 28) are more widely distributed. It is thought that matrilins have an adapter function in the extracellular matrix, connecting macromolecular networks (14). This role for matrilins was confirmed by recent results showing that matrilin-1, matrilin-3, and matrilin-4 associated with collagen VI microfibrils extracted from rat chondrosarcoma tissue and connected these fibrils to aggrecan and collagen II (30). The matrilins are bound to the small leucine-rich repeat proteoglycans biglycan and decorin, which in turn interact with the N-terminal globular domains of the collagen VI molecules.

Monomeric matrilin-3 is the simplest member of the matrilin family, consisting of only one vWFA domain followed by four EGF-like domains and a C-terminal coiled-coil domain (27). A second vWFA domain, present in the other matrilins between the EGF-like domains and the coiled-coil domain, is absent. Matrilin-3 can form homotetramers via the coiled-coil domain (16), and in addition, mixed trimers and tetramers of matrilin-3 and matrilin-1 have been observed in human (19) and calf (16, 32), whereas these heterooligomers could not be identified in mouse (3).

In mouse, matrilin-3 is expressed in dense connective tissue during growth and remodelling, with earliest detection at day 12.5 postcoitus in cartilage anlagen of the developing bones. In newborn mice, matrilin-3 is abundant in the developing occipital bones and the bones of the nasal cavity, the cartilage primordium of the vertebral bodies, the ribs, and the long bones, as well as in the sternum and trachea (16, 18). In 6-week-old mice, the expression is restricted to the growth plates of long bones, sternum and vertebrae (18), and the tracheal perichondrium (16). When present, matrilin-3 colocalizes with matrilin-1 except in a region adjacent to the resting cartilage of the developing joint, where only matrilin-3 can be detected. Matrilin-3 expression gradually ceases after birth, while matrilin-1 remains in cartilage throughout life (18).

Matrilin-3 is highly upregulated in human osteoarthritic cartilage (24), and a missense mutation in the human matrilin-3 gene was recently found to coincide with hand osteoarthritis in a group of patients in the Icelandic population (25). Other mutations in matrilin-3 have been shown to cause multiple epiphyseal dysplasia (MED), a form of osteochondrodysplasia characterized by delayed and irregular ossification of the epiphyses and early-onset osteoarthritis (6, 7), and bilateral hereditary microepiphyseal dysplasia, a MED-like disorder characterized by small epiphyses in the hip and the knee joint (22). It is still not clear if these diseases are caused by a loss of matrilin-3 function or by a dominant-negative effect of the mutant protein on chondrocyte viability or extracellular matrix assembly.

Matrilin-1 is the only family member thus far described to have been inactivated by gene targeting in mouse (3, 15). While in one case (15), minor alterations in cartilage collagen fibrillogenesis and fibril organization were reported, neither of the two mouse lines produced showed gross morphological changes.

---

* Corresponding author. Mailing address: Department of Molecular Medicine, Max Planck Institute for Biochemistry, Am Klopferspitz 18A, 82152 Martinsried, Germany. Phone: 49-89-8578-2849. Fax: 49-89-8578-2422. E-mail: aszodi@biochem.mpg.de.

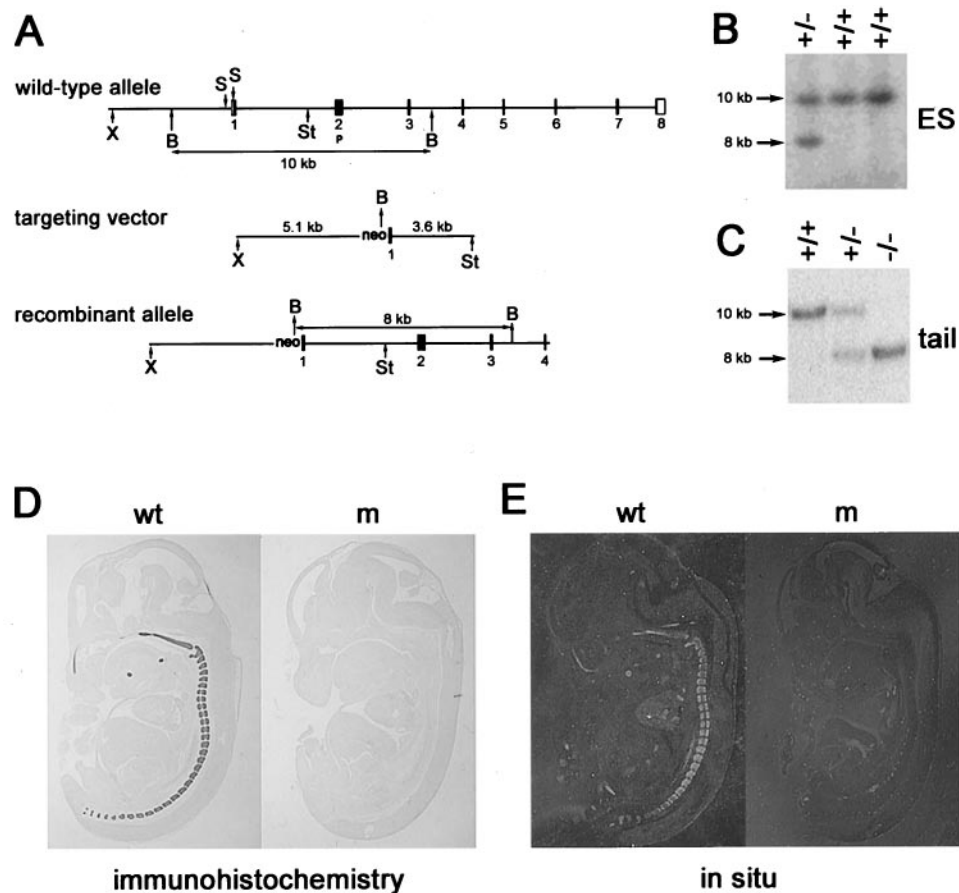† B.K. and C.N. contributed equally to this work.

FIG. 1. Targeted disruption of mouse *Matn-3*. (A) Structure of the mouse *Matn3* gene, targeting construct, and targeted allele after homologous recombination. Black and open boxes indicate the translated and untranslated regions of exons (E1 to E8), respectively. The expected fragment sizes for wild-type and targeted alleles are 10 and 8 kb, respectively, following digestion with *Bst*XI and hybridization with the indicated external probe (p). neo, neomycin cassette. (B) Southern blot analysis of genomic DNA from ES cell clones shows the wild-type (10 kb) and the targeted (8 kb) alleles. (C) Southern blot analysis of tail DNA isolated from a mouse homozygous for the wild-type allele (+/+), a heterozygous mouse (+/−), and a homozygous mutant mouse (−/−). (D) Immunohistochemistry using a matrilin-3-specific antibody on tissue sections from embryonic day 13.5 embryo confirms the lack of matrilin-3 in the mutant. m, mutant; wt, wild type. (E) In situ hybridization shows the absence of matrilin-3 mRNA in a homozygous mutant embryo.

In the present study, we report on the targeted disruption of the *Matn-3* gene encoding matrilin-3 in mice. Both heterozygous and homozygous mutant mice are viable and show no detectable abnormalities. Our results carry the implication that human disease due to matrilin-3 mutations is caused not by a loss of matrilin-3 but by the mutant protein being deleterious to cell or tissue function.

MATERIALS AND METHODS

Generation of matrilin-3-deficient mice. A 10-kb genomic fragment harboring the first exon of the mouse *Matn-3* gene was isolated from a 129/Sv genomic library as described previously (29). *Matn-3* was disrupted by inserting the phosphoglycerate kinase-neomycin cassette into *Sma*I sites, leading to the deletion of the ATG-containing 5′ part of exon 1 (Fig. 1A). The targeting vector, containing a 5.1-kb right arm and a 3.6-kb left arm, was linearized by *Not*I digestion, electroporated into R1 embryonic stem (ES) cells, and subjected to G418 selection (500 μg/ml in ES cell medium). To check for homologous recombination, *Bst*XI-digested genomic DNA was analyzed by Southern blotting using a 400-bp external probe. This probe identifies a 10-kb fragment and an 8-kb fragment in the wild-type and mutant alleles, respectively. The correctly targeted ES cells were injected into blastocysts to generate chimeras. Male chimeras were subsequently mated with C57BL/6 females, and germ line transmission of the mutant

allele was demonstrated by Southern analysis of tail DNA using the external probe.

Skeletal staining and X-ray analysis. Newborn specimens were deskinned and eviscerated, fixed in 95% ethanol for 3 days, and then transferred into acetone for 1 day. Staining was performed in a solution of 90% ethanol, 5% acetic acid, and 5% H_2O supplemented with 0.005% alizarin red S (Sigma) and 0.015% alcian blue 8GS (Sigma) for 3 days at 37°C. Samples were rinsed in water and cleared for 3 days in 1% potassium hydroxide followed by clearing in 0.8% KOH–20% glycerol for 1 week. Samples were then transferred into 50, 80, and finally 100% glycerol for long-term storage. For X-ray analysis, 1-year-old control and *Matn-3* null mice were anesthetized and images were taken with a Siemens Polymat 70 at 48 kV, 0.2 mA.

Histology and immunohistochemistry. For histological analysis, specimens of various pre- and postnatal stages were fixed overnight in 4% paraformaldehyde (PFA) in phosphate-buffered saline (PBS), pH 7.4. Samples taken after birth were decalcified in 10% EDTA–PBS for 1 to 2 weeks. After embedding in paraffin, sections of 6 to 8 μm were cut and stained with hematoxylin-eosin (HE), safranin orange-van Kossa, or safranin orange-Weigert hematoxylin-methyl green according to the standard histochemical protocols.

For immunostainings, specimens were fixed in 95% ethanol–1% acetic acid overnight at 4°C, decalcified if needed, and embedded into paraffin. Immunohistochemistry was conducted with hyaluronidase-treated 6-μm-thick sections using the Vectastain ABC Elite kit (Vector Laboratories) and using 3,3′-diaminobenzidine (Sigma) as the chromogenic substrate. Primary antibodies to the

following antigens were used: collagen type II (obtained from Rickard Holm-dahl, Lund University, Lund, Sweden), collagen type X (a gift from Björn R. Olsen, Harvard Medical School, Harvard University, Boston, Mass.), endomucin (4), matrilin-1 (13), matrilin-2 (23), matrilin-3 (16), and matrilin-4 (17). Antibodies were affinity purified, as necessary, by binding to the antigen coupled to Sepharose followed by elution at acidic pH.

In vivo chondrocyte proliferation was monitored by the BrdU incorporation assay. Mice were injected intraperitoneally with BrdU (50 μg/g of body weight in PBS). After 1 h, the mice were killed and samples were dissected, fixed, and embedded into paraffin. Deparaffinized sections were treated with 2 M HCl for 30 min, washed in PBS, and incubated with a peroxidase-conjugated antibody to BrdU (clone BMG-6H8; dilution, 1:33; Roche) for 1 h in PBS–1% bovine serum albumin–0.25% Tween 20. Following washes in PBS, detection was performed with 3,3′-diaminobenzidine solution. Cell death was analyzed using the in situ cell death detection kit (Roche) according to the instructions of the manufacturer.

RNA isolation, Northern blot analysis, and in situ hybridization. Total RNA was isolated from newborn limb chondrocytes with the Qiagen RNeasy kit according to the instructions of the manufacturer. For Northern analysis, 5 μg of total RNA was size fractionated on a 1% agarose–2.2 M formaldehyde gel and blotted to a Hybond XL membrane (Amersham). The membrane was consecutively hybridized with ^{32}P-labeled cDNA probes specific for mouse *Matn-1*, *Matn-2*, *Matn-3*, *Matn-4* (3, 26), or *Gapdh* (glyceraldehyde phosphodehydrogenase gene).

Nonradioactive in situ hybridization on tissue sections for mouse collagen II (*Col2a1*), collagen X (*Col10a1*), Indian hedgehog (*Ihh*), and Parathyroid hormone/Parathyroid hormone-related peptide receptor (*Ppr*) mRNA was performed as described by Brandau et al. (5). Briefly, newborn limbs were fixed in 4% PFA in Tris-buffered saline (TBS) (pH 9.5) and subsequently dehydrated and embedded in paraffin. Six-micrometer-thick sections were dewaxed, rehydrated, rinsed in TBS (pH 7.4), and postfixed with 4% PFA-TBS (pH 9.5) for 10 min. Sections were rinsed in TBS (pH 7.4), treated with 10 μg of proteinase K/ml for 30 min at 37°C, acetylated with 0.25% acetic anhydride for 10 min, washed three times in TBS (pH 7.4), and dehydrated in an ascending ethanol series. Air-dried sections were hybridized with digoxigenin-UTP-labeled antisense riboprobes overnight at 52°C. After hybridization, sections were washed three times for 30 min each at 55°C in 50% formamide, 2× sodium citrate-chloride buffer (SSC [1× SSC is 0.015 M sodium citrate and 0.15 M NaCl]), and twice in 1× SSC for 15 min at room temperature. The sections were then incubated with an alkaline phosphatase-coupled antibody against digoxigenin (Roche) diluted 1:500 in TBS (pH 7.4) containing 2% sheep serum and 0.1% Triton X-100 for 2 h at room temperature. After rinsing in TBS (pH 7.4), color detection was performed according to the recommendation of the manufacturers. Radioactive in situ hybridization was performed as described previously (2) using [P^{33}]UTP-labeled riboprobes against *Matn-3*.

Ultrastructural analysis. The proximal tibia of newborn wild-type and homozygous mutant animals was dissected and fixed in 0.1 M cacodylate buffer (pH 7.4), supplemented with 2% glutaraldehyde, for 2 days. The specimens were further processed for the ultrastructural investigation as previously described (21). Micrographs were taken with the help of an electron microscope (Leo 906E; Zeiss, Oberkochen, Germany).

Cartilage extraction, SDS-polyacrylamide gel electrophoresis (PAGE), and immunoblotting. Knee joints and sterna were weighed and frozen at −80°C. On the day of extraction, the specimens were cut into 1-mm³ pieces. Ten volumes (milliliter per gram of wet tissue) of chilled buffer I (0.15 M NaCl, 50 mM Tris [pH 7.4]) were added, and the tissue was extracted for 7 to 10 h at 4°C with continuous mixing. The extracts were clarified by centrifugation, and the supernatants were stored at −20°C. The pellets were reextracted in an identical manner with buffer II (1 M NaCl, 10 mM EDTA, 50 mM Tris [pH 7.4]), and the remaining insoluble material was extracted with buffer III (4 M GuHCl, 10 mM EDTA, 50 mM Tris [pH 7.4]). All extraction buffers contained 2 mM phenylmethylsulfonyl fluoride and 2 mM N-ethylmaleimide.

One-hundred-microliter aliquots of the extracts obtained with buffers I, II, and III were precipitated with 1 ml of 96% ethanol overnight at 4°C. The precipitates were washed with a mixture of 9 vol of 96% ethanol and 1 vol of TBS for 2 h at 4°C with gentle agitation. After centrifugation, the pellets were air dried and suspended in 150 μl of water, and the same volume of 2× nonreducing SDS-PAGE sample buffer was added. Aliquots were applied to 4 to 15% SDS-polyacrylamide gels. SDS-PAGE was performed as described by Laemmli (20). For immunoblots, the proteins were transferred to nitrocellulose and incubated with the appropriate affinity-purified rabbit antibodies (see immunohistochemistry) diluted in TBS. Bound antibodies were detected by luminescence using the peroxidase-conjugated swine anti-rabbit immunoglobulin G (Dako), 3-aminopthalhydrazide (1.25 mM), p-coumaric acid (225 μM), and 0.01% H$_2$O$_2$.

Other aliquots of the extracts were analyzed for glycosaminoglycan content by the dimethylmethylene blue assay (12).

RESULTS

Generation of matrilin-3-deficient mice. *Matn-3* was inactivated by homologous recombination in ES cells, partially deleting the promoter region and the 5′ part of exon 1 carrying the translational initiation codon, ATG (Fig. 1A). Out of 360 ES cell clones surviving the G418 selections, eight correctly targeted clones were identified by Southern blot analysis of *Bst*XI-digested genomic DNA using an external probe (Fig. 1B). ES cells from two targeted clones were used to generate germ line chimeric males, which were subsequently mated with C57BL/6 females to generate heterozygous offspring. Heterozygous breeding produced wild-type, heterozygous, and mutant offspring (Fig. 1C) in a normal Mendelian ratio (results not shown). The null mutation was confirmed on tissue sections at embryonic day 13.5. Immunohistochemistry using an affinity-purified rabbit polyclonal antibody against matrilin-3 and in situ hybridization using an antisense RNA probe demonstrated the complete absence of the matrilin-3 protein and mRNA in homozygous mutant mice, respectively (Fig. 1D and E).

Gross morphology of the skeleton is normal in *Matn-3* null mice. Matrilin-3-deficient mice showed no obvious abnormalities, were fertile, and had normal life spans. Since matrilin-3 is expressed by chondrocytes and osteoblasts during endochondral bone formation (16), we first analyzed the gross skeletal morphology of newborn and adult mutant mice.

Whole-mount staining with alcian blue (for cartilage) and alizarin red (for bone) of newborn mice revealed that all bones of the appendicular, axial, and craniofacial skeleton formed normally in *Matn-3* null mice (Fig. 2A). A closer view of the limbs (Fig. 1B), rib cage (Fig. 2C), trunk region (Fig. 2D), and the base of the skull (Fig. 2E) showed no evidence of size reduction or any malformation in mutants compared to controls. Furthermore, careful measurement of the length of skeletal elements of the hind limbs and forelimbs demonstrated no significant difference between homozygous mutant mice and wild-type mice (Fig. 2F). Finally, X-ray analysis of 12-month-old control and matrilin-3-deficient animals did not show any skeletal abnormalities (Fig. 2G).

Taken together, these data indicate that the lack of matrilin-3 has no impact on normal skeletal growth.

Matrilin-3-deficient mice show normal endochondral bone formation and intervertebral disk development. To investigate the skeletal development of the *Matn-3* null mice in greater detail, we performed histological, immunohistological, in situ hybridization, and ultrastructural analyses. HE staining of tissue sections of long bones at newborn stage revealed normal cartilage organization and growth plate architecture in null mice (Fig. 3A). In addition, the appearance of the long bones at various adult stages was identical in wild-type and mutant mice (Fig. 3B and data not shown). Safranin orange staining for proteoglycans up to 9 months of age showed no sign of degenerative changes of the articular cartilage in mutants (Fig. 3B and data not show). Similar to that of long bones, the
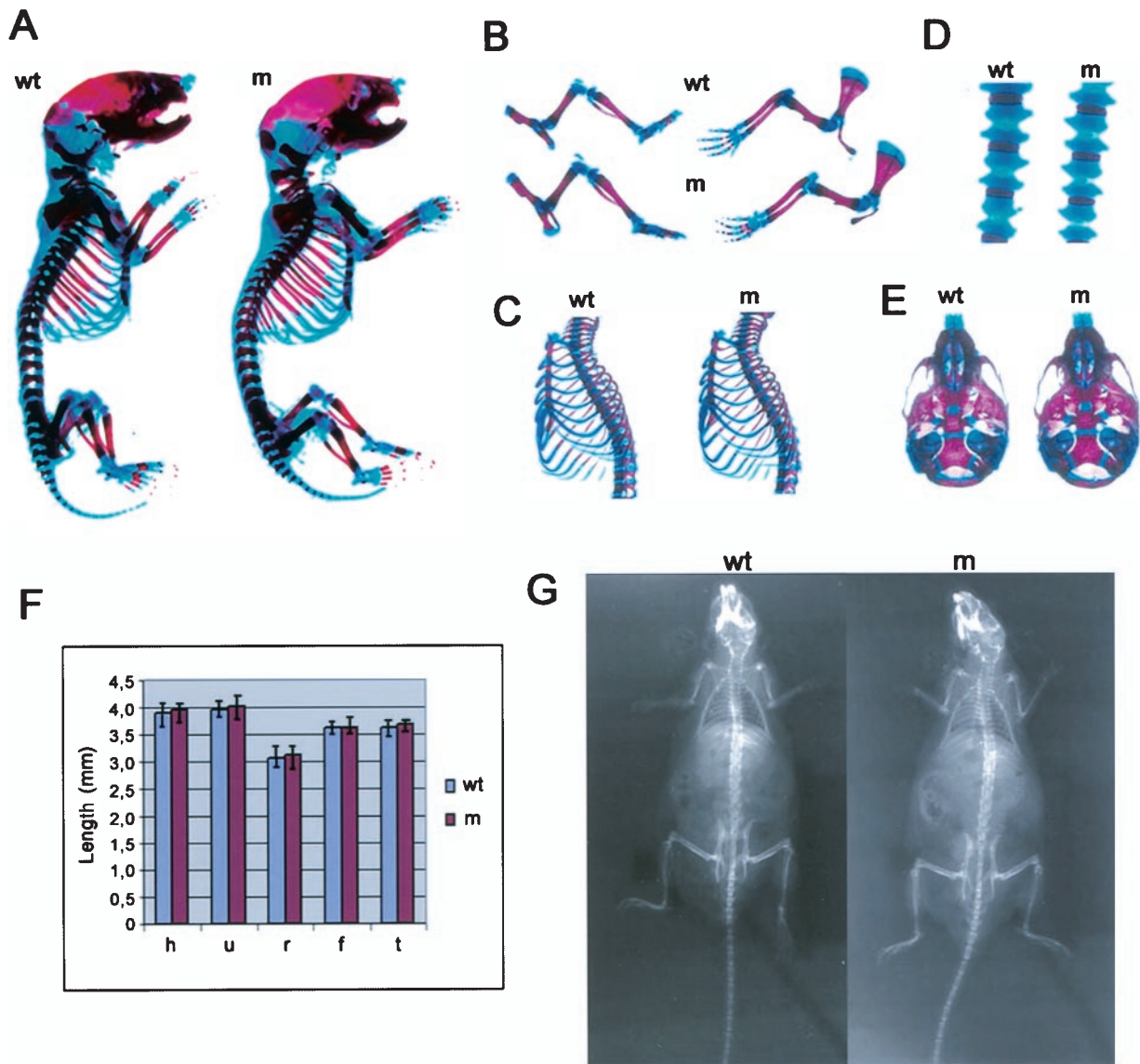
FIG. 2. Analysis of the skeletal anatomy in wild-type and matrilin-3-deficient mice. (A) Whole-mount staining shows that newborn mutant (m) mice have a skeletal structure that does not differ from that of wild-type (wt) mice. The size and the appearance of the long bones of the limbs (B), rib cage (C), trunk (D), and the base of the skull (E) are indistinguishable between wild-type and mutant littermates. (F) There is no statistically significant difference in the length of the long bones of newborn limbs between wild-type and mutant mice ($n = 5$). Error bars represent ± standard errors of the mean. Abbreviations: h, humerus; u, ulna; r, radius; f, femur; t, tibia. (G) X-ray analysis of 12-month-old wild-type and mutant mice shows no difference in skeletal morphology.

development of the ribs, vertebral bodies, and intervertebral disks was normal in *Matn-3* null mice (Fig. 3D and data not shown). Ultrastructural analysis of epiphyseal and growth plate cartilages of newborn femur and tibia showed normal chondrocyte morphology and the presence of a normal collagen fibrillar network in the extracellular matrix (Fig. 3G).

Next, we investigated markers for chondrocyte differentiation in the mutant long bones. Immunostaining of the humerus from newborn mice showed the normal deposition of the typical cartilage proteins, including collagen II, collagen X, and aggrecan (Fig. 4A). In situ hybridization of tibial sections with riboprobes for *Col2a1*, *Col10a1*, *Ihh*, and *Ppr* revealed a nor-

mal differentiation of mutant growth plate chondrocytes (Fig. 4B and data not shown). Van Kossa staining of newborn tibias for mineralized tissues indicated that the formation of the cortical and trabecular bones occurs normally in mutants (Fig. 4C). Staining for alkaline phosphatase and tartrate-resistant acid phosphatase activity showed normal numbers of osteoblasts and osteoclasts, respectively (Fig. 4D and E). The vascular invasion front of the growth plate cartilage was investigated by immunostaining for endomucin as a marker for endothelial cells (4). We observed no difference in vascularization between wild-type and mutant growth plates (Fig. 4F). Finally, no changes in chondrocyte proliferation or apoptosis
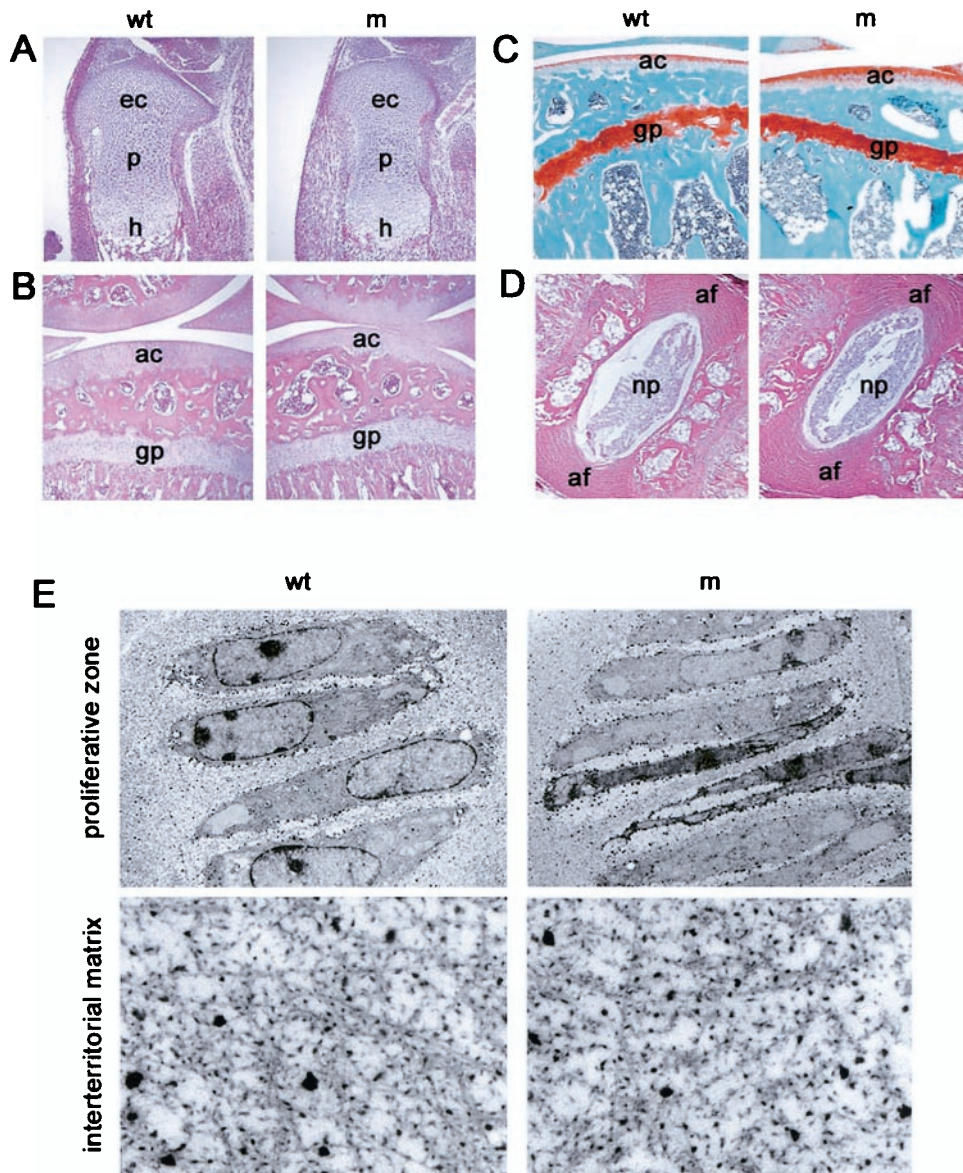
FIG. 3. Histological and ultrastructural analysis of skeletal development. HE staining of the proximal part of the tibia from newborn wild-type (wt) and mutant (m) mice (A) and the knee region from 8-week-old mice (B) shows comparable size and ultrastructure between control and mutant. (C) Safranin orange staining of the tibial head at 9 months of age gives no indication of degenerative changes in the articular cartilage in mutants. (D). HE staining shows normal intervertebral disk formation in mutants. (E) Electron microscopy revealed no abnormalities in chondrocyte morphology or collagen fibrillar network organization in mutant growth plate cartilage. Abbreviations: ec, epiphyseal cartilage; p, proliferative zone of the growth plate; h, hypertrophic zone of the growth plate; gp, growth plate; ac, articular cartilage; np, nucleus pulposus; af, annulus fibrosus.

rate could be detected as measured by BrdU incorporation and terminal deoxynucleotidyltransferase-mediated dUTP-biotin nick end labeling assay, respectively (results not shown).

Normal expression of other members of the matrilin family in matrilin-3-deficient skeletal tissues. To address the question of whether the lack of an apparent skeletal phenotype in the *Matn-3* null mice is due to compensation by structurally and functionally related proteins, we analyzed the expression of other members of the matrilin family using various methods. Northern hybridization of total RNA isolated from newborn limb cartilage demonstrated that the steady-state levels of

Matn-1, *Matn-2*, and *Matn-4* mRNAs were not significantly altered in mutant mice compared to those in wild-type mice (Fig. 5A and B). Immunostaining of newborn tibias with a matrilin-3-specific antiserum showed the absence of Matn-3 and the normal deposition of Matn-1, Matn-2, and Matn-4 in mutant cartilage (Fig. 6). Similarly, no differences between wild-type and mutant mice were revealed by biochemical analysis of cartilage samples at the newborn stage. Cartilage proteins were sequentially extracted from sternal and knee cartilage with neutral salt (fraction I), high salt with 10 mM EDTA (fraction II), and 4 M GuHCl (fraction III). Western blot
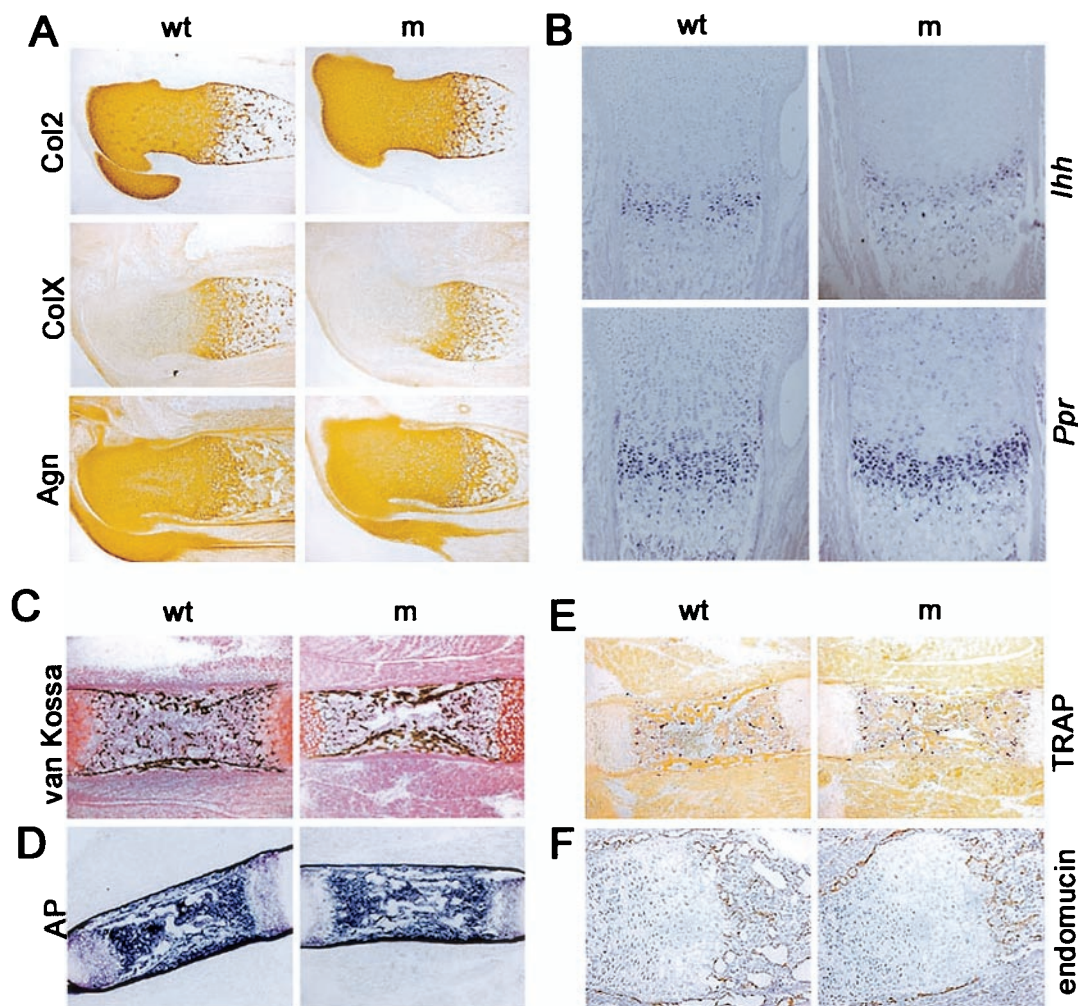
FIG. 4. Cartilage differentiation and bone development are normal in *Matn-3* null mice. (A) Immunohistochemistry shows normal deposition of cartilage-specific proteins. Consecutive sections of the humerus from wild-type (wt) and mutant (m) mice were stained with antibodies against type II collagen (Col2), aggrecan (Agn), and type X collagen (ColX). (B) In situ hybridization with probes specific for *Ihh* and *Ppr* mRNA shows similar expression of these growth plate differentiation markers in wild-type and mutant newborn tibial sections. (C) Van Kossa staining indicates normal mineral deposition in the tibia of newborn mutant mice. The sections were counterstained with safranin orange. (D) Alkaline phosphatase histochemistry (blue staining) shows that differentiation and activity of osteoblasts are normal in mutant mice. (E) Staining for tartrate-resistant acid phosphatase (TRAP) activity (red staining) indicates comparable numbers of osteoclasts in wild-type and mutant long bones. (G) Immunostaining for endomucin, a marker for vascular endothelial cells, shows a normal vascular invasion front in the mutant growth plate.

analysis after nonreducing SDS-PAGE indicated that in wild-type cartilage, Matn-1, Matn-3, and Matn-4 were present in fractions II and III, whereas Matn-2 was detectable in all three fractions (Fig. 7A and B). In mutant samples, Matn-3 was absent while the amounts of Matn-1, Matn-2, Matn-4, collagen type II, and cartilage oligomeric matrix protein (COMP) were comparable with those of the control (Fig. 7B). Furthermore, dimethylmethylene blue assay of cartilage extracts indicated no difference in glycosaminoglycan content between wild-type and mutant cartilages (data not shown).

DISCUSSION

It has been proposed that matrilins play an important structural role in extracellular matrices, forming self-assembled filamentous networks. In cartilage, all four members of the ma-

trilin family are expressed, suggesting important biological role(s) for matrilins in this tissue. Studies with chondrosarcoma cell lines or primary chondrocytes revealed that matrilin-3/matrilin-1 networks connect neighboring cells in a collagen-dependent manner, whereas in the pericellular matrix, these matrilins form collagen-independent filaments (8, 9, 16). Matrilin-1, the best-characterized matrilin, interacts periodically with type II collagen fibrils (31) and binds covalently to aggrecan (14), forming a bridge between the two major supramolecular components of the cartilage. Based on structural similarities, this bridging, or adaptor, function was suggested as a common feature of all matrilins (10). A very recent study with the Swarm rat chondrosarcoma indicates that the actual interactions between matrilins and other cartilage matrix proteins might be even more complicated. It has been shown that matrilin-1, matrilin-3, and matrilin-4 form complexes with the
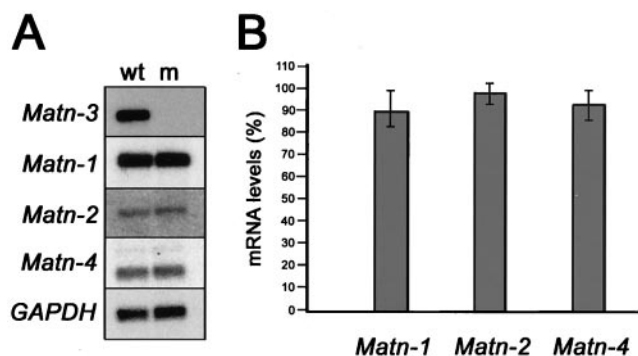
FIG. 5. Northern blot analysis. (A) A representative Northern blot analysis of total RNA isolated from wild-type (wt) and mutant (m) newborn limb cartilage. The filter was consecutively hybridized with probes specific for *Matn1-4* and *Gapdh*. (B) Diagram showing the percentage of *Matn1*, *Matn2*, and *Matn4* mRNA levels in the mutant compared to that of the wild type ($n = 3$). The hybridization intensities were normalized to the amount of *Gapdh* mRNA. Error bars represent ± standard errors of the mean.

small leucine-reach repeat proteoglycans decorin and biglycan, which bind to the N termini of collagen type VI and, at least in the case of matrilin-1, link collagen VI microfibrils to aggrecan or collagen II (30).

The biological relevance of such matrilin-cartilage extracellular matrix protein interactions is not clear. Matrilin-1-deficient mice have no obvious skeletal defects (3, 15), and in this paper we demonstrate that mice lacking matrilin-3 are indistinguishable from wild-type mice and display normal cartilage and bone development. Deposition of cartilage matrix proteins, such as collagen II and aggrecan, terminal differentiation process of the chondrocytes, growth plate structure, and replacement of cartilage by bone all remain unaltered in these mutants. In contrast to *Matn-1* null mice, which show a mild defect in collagen fibril organization in the maturation and hypertrophic zone of the growth plate (15), we observed no ultrastructural abnormalities in Matn-3-deficient mice. These

data suggest that the presence of matrilin-3 in the cartilage and bone is not important for skeletal development and the proper assembly of the extracellular matrix.

The lack of apparent phenotype in matrilin-3 null cartilage could be explained by the expression of other members of the matrilin family in skeletal tissues. Matrilin-3 is coexpressed with matrilin-1 and matrilin-4 in the resting, proliferative, and hypertrophic zones of the developing knee joint, and all four matrilins are expressed in the proliferative and upper hypertrophic zones (18) (Fig. 6). Similarly, matrilin-3 is coexpressed with at least one other matrilin in the articular, sternal, costal, and vertebral cartilage and the inner part of the annulus fibrosus of the intervertebral disk (18). Northern blot, immunohistochemical, and biochemical analyses of newborn knee joint or sternal cartilage did not reveal a compensatory up-regulation of *Matn*-1, *Matn*-2, or *Matn*-4 in *Matn*-3 null mice, but redundancy between matrilin-3 and, especially, matrilin-1 and/or matrilin-4 cannot be excluded. Such a redundancy among matrilins was already suggested to explain the lack of an overt phenotype in the matrilin-1-deficient mice (3, 15).

Mutations in extracellular matrix proteins expressed in cartilage frequently lead to human osteochondrodysplasias with various degrees of severity. To date, matrilin-3 is the only known member of the matrilin family found to be associated with such disorders. A mild form of the autosomal dominant MED is caused by missense mutations (V194D and R121D) in the second exon of the *MATN3* gene encoding the vWFA domain (7). Another missense mutation in the same region of MATN3 (A128P) was discovered recently in a family with bilateral hereditary microepiphyseal dysplasia, which is known to be a distinct variant form of MED (22). These mutations were suggested to alter the folding and/or function of the vWFA domain, indicating that the disorder is most probably due to a dominant-negative effect rather than being caused by haploinsufficiency (6, 7). This hypothesis is further strengthened by the observation that a single nucleotide deletion in *MATN3*, which creates a premature stop codon at amino acid residue 164, has no pathophysiological consequence (6). The lack of a
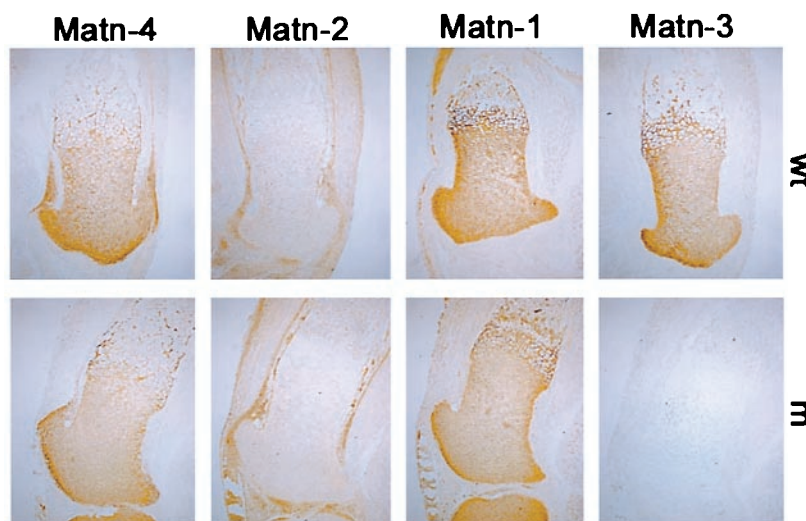

FIG. 6. Immunohistochemical staining of developing bones for matrilins. Newborn tibias from wild-type (wt) and homozygous mutant (m) mice were immunostained with polyclonal antibodies against Matn-1, Matn-2, Matn-3, and Matn-4.
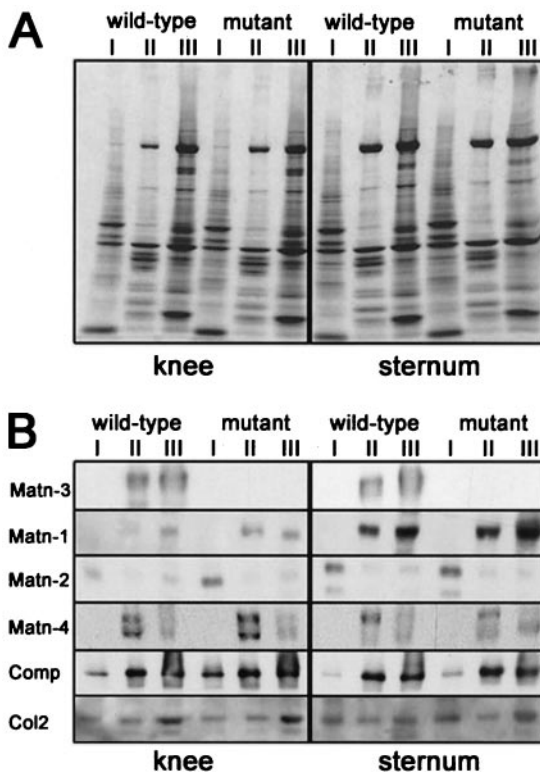
FIG. 7. Biochemical analysis of wild-type and mutant knee joint and sternal cartilages. (A) Coomassie-stained SDS-polyacrylamide gel of proteins sequentially extracted with buffer I, buffer II, and buffer III (see Materials and Methods) from newborn knee joint and sternal cartilage. (B) Western blot analysis of wild-type and mutant knee joint and sternal samples for matrilin-1, matrilin-2, matrilin-3, and matrilin-4 and for COMP and collagen II.

chondrodysplasia phenotype in the matrilin-3-deficient mice is in line with this finding and strongly supports dominant-negative action as the pathomechanism of MED.

A similar contrast between the null mutation in mice and the human disorder was recently described for COMP. COMP-deficient mice are normal and display no detectable skeletal defects (26). Mutations in the human *COMP* gene, however, lead to MED and the clinically more severe pseudoachondroplasia (6). Most of these mutations cause conformational changes of COMP, resulting in its reduced secretion and accumulation in the rough endoplasmatic reticulum. The misfolded COMP molecules, in turn, retain other matrix proteins, including collagen type IX, decorin, and aggrecan, in the rough endoplasmatic reticulum, leading to reduced cell viability due to this accumulation of intracellular protein (11). Whether or not the MATN3-related disorders are caused by a mechanism similar to that in the case of COMP remains to be elucidated.

In summary, our results show that the absence of matrilin-3 in mice has no impact on endochondral bone formation and indicate that loss-of-function mutation(s) in the matrilin-3 gene cannot account for MED and MED-like disorders seen in humans. Generation of multiple-knockout mice or mice carrying dominant-negative mutations might be necessary to clarify the function of matrilins in skeletal development.

REFERENCES

1. **Aszódi, A., N. Hauser, D. Studer, M. Paulsson, L. Hiripi, and Z. Bösze.** 1996. Cloning, sequencing and expression analysis of mouse cartilage matrix protein cDNA. Eur. J. Biochem. **236:**970–977.
2. **Aszódi, A., D. Chan, E. Hunziker, J. F. Bateman, and R. Fässler.** 1998. Collagen II is essential for the removal of the notochord and the formation of intervertebral discs. J. Cell Biol. **143:**1399–1412.
3. **Aszódi, A., J. F. Bateman, E. Hirsch, M. Baranyi, E. B. Hunziker, N. Hauser, Z. Bösze, and R. Fässler.** 1999. Normal skeletal development of mice lacking matrilin 1: redundant function of matrilins in cartilage? Mol. Cell. Biol. **19:**7841–7845.
4. **Brachtendorf, G., A. Kuhn, U. Samulowitz, R. Knorr, E. Gustafsson, A. J. Potocnik, R. Fässler, and D. Vestweber.** 2001. Early expression of endomucin on endothelium of the mouse embryo and on putative hematopoietic clusters in the dorsal aorta. Dev. Dyn. **222:**410–419.
5. **Brandau, O., A. Aszódi, E. B. Hunziker, P. J. Neame, D. Vestweber, and R. Fässler.** 2002. Chondromodulin is dispensable during endochondral ossification and eye development. Mol. Cell. Biol. **22:**6627–6635.
6. **Briggs, M. D., and K. L. Chapman.** 2002. Pseudoachondroplasia and multiple epiphyseal dysplasia: mutation review, molecular interactions, and genotype to phenotype correlations. Hum. Mutat. **19:**465–478.
7. **Chapman, K. L., G. R. Mortier, K. Chapman, J. Loughlin, M. E. Grant, and M. D. Briggs.** 2001. Mutations in the region encoding the von Willebrand factor A domain of matrilin-3 are associated with multiple epiphyseal dysplasia. Nat. Genet. **28:**393–396.
8. **Chen, Q., D. M. Johnson, D. R. Haudenschild, M. M. Tondravi, and P. F. Goetinck.** 1995. Cartilage matrix protein forms a type II collagen-independent filamentous network: analysis in primary cell cultures with a retrovirus expression system. Mol. Biol. Cell **6:**1743–1753.
9. **Chen, Q., Y. Zhang, D. M. Johnson, and P. F. Goetinck.** 1999. Assembly of a novel cartilage matrix protein filamentous network: molecular basis of differential requirement of von Willebrand Factor A domains. Mol. Biol. Cell **10:**2149–2162.
10. **Deák, F., R. Wagener, I. Kiss, and M. Paulsson.** 1999. The matrilins: a novel family of oligomeric extracellular matrix proteins. Matrix Biol. **18:**55–66.
11. **Dinser, R., F. Zaucke, F. Kreppel, K. Hultenby, S. Kochanek, M. Paulsson, and P. Maurer.** 2002. Pseudoachondroplasia is caused through both intra- and extracellular pathogenic pathways. J. Clin. Investig. **110:**505–513.
12. **Farndale, R. W., D. J. Buttle, and A. J. Barrett.** 1986. Improved quantitation and discrimination of sulphated glycosaminoglycans by use of dimethylmethylene blue. Biochim. Biophys. Acta **883:**173–177.
13. **Hauser, N., and M. Paulsson.** 1994. Native cartilage matrix protein (CMP). A compact trimer of subunits assembled via a coiled-coil α-helix. J. Biol. Chem. **269:**25747–25753.
14. **Hauser, N., M. Paulsson, D. Heinegård, and M. Mörgelin.** 1996. Interaction of cartilage matrix protein (CMP) with aggrecan. Increased covalent crosslinking with maturation. J. Biol. Chem. **271:**32247–32252.
15. **Huang, X., D. E. Birk, and P. F. Goetinck.** 1999. Mice lacking matrilin-1 (cartilage matrix protein) have alterations in type II collagen fibrillogenesis and fibril organization. Dev. Dyn. **216:**434–441.
16. **Klatt, A. R., P. D. Nitsche, B. Kobbe, M. Mörgelin, M. Paulsson, and R. Wagener.** 2000. Molecular structure and tissue distribution of matrilin-3, a filament-forming extracellular matrix protein expressed during skeletal development. J. Biol. Chem. **275:**3999–4006.
17. **Klatt, A. R., D. P. Nitsche, B. Kobbe, M. Macht, M. Paulsson, and R. Wagener.** 2001. Molecular structure, processing, and tissue distribution of matrilin-4. J. Biol. Chem. **276:**17267–17275.
18. **Klatt, A. R., M. Paulsson, and R. Wagener.** 2002. Expression of matrilins during maturation of mouse skeletal tissues. Matrix Biol. **21:**289–296.
19. **Kleemann-Fischer, D., G. R. Kleemann, D. Engel, J. R. Yates III, J. J. Wu, and D. R. Eyre.** 2001. Molecular properties of matrilin-3 isolated from human growth cartilage. Arch. Biochem. Biophys. **387:**209–215.
20. **Laemmli, U. K.** 1970. Cleavage of structural proteins during the assembly of the head of bacteriophage T4. Nature **227:**680–685.
21. **Miosge, N., C. Klenczar, R. Herken, M. Willem, and U. Mayer.** 1999. Orga-

nization of the myotendinous junction is dependent on the presence of alpha7beta1 integrin. Lab. Investig. **79:**1591–1599.

22. **Mostert, A. K., P. F. Dijkstra, B. R. H. Jansen, J. R. van Horn, B. de Graaf, P. Heutink, and D. Lindhout.** 2003. Familial multiple epiphyseal dysplasia due to a matrilin-3 mutation: further delineation of the phenotype including 40 years follow-up. Am. J. Med. Genet. **120A:**490–497.

23. **Piecha, D., S. Muratoglu, M. Mörgelin, N. Hauser, D. Studer, I. Kiss, M. Paulsson, and F. Deak.** 1999. Matrilin-2, a large, oligomeric matrix protein, is expressed by a great variety of cells and forms fibrillar networks. J. Biol. Chem. **274:**13353–13361.

24. **Pullig, O., G. Weseloh, A. R. Klatt, R. Wagener, and B. Swoboda.** 2002. Matrilin-3 in human articular cartilage: increased expression in osteoarthritis. Osteoarthritis Cartilage **10:**253–263.

25. **Stefansson, S. E., H. Jonsson, T. Ingvarsson, I. Manolescu, H. H. Jonsson, G. Olafsdottir, E. Palsdottir, G. Stefansdottir, G. Sveinbjornsdottir, M. L. Frigge, A. Kong, J. R. Gulcher, and K. Stefansson.** 2003. Genomewide scan for hand osteoarthritis: a novel mutation in matrilin-3. Am. J. Hum. Genet. **72:**1448–1459.

26. **Svensson, L., A. Aszódi, D. Heinegard, E. Hunziker, F. P. Reinholt, R. Fässler, and A. Oldberg.** 2002. Cartilage oligomeric matrix protein-deficient mice have normal skeletal development. Mol. Cell. Biol. **22:**4366–4371.

27. **Wagener, R., B. Kobbe, and M. Paulsson.** 1997. Primary structure of matrilin-3, a new member of a family of extracellular matrix proteins related to cartilage matrix protein (matrilin-1) and von Willebrand factor. FEBS Lett. **413:**129–134.

28. **Wagener, R., B. Kobbe, and M. Paulsson.** 1998. Matrilin-4, a new member of the matrilin family of extracellular matrix proteins. FEBS Lett. **436:**123–127.

29. **Wagener, R., B. Kobbe, A. Aszódi, Z. Liu, D. R. Beier, and M. Paulsson.** 2000. Structure and mapping of the mouse matrilin-3 gene (*Matn3*), a member of a gene family containing a U12-type AT-AC intron. Mamm. Genome **11:**85–90.

30. **Wiberg, C., A. R. Klatt, R. Wagener, M. Paulsson, J. F. Bateman, D. Heinegård, and M. Mörgelin.** 2003. Complexes of matrilin-1 and biglycan or decorin connect collagen VI microfibrils to both collagen II and aggrecan. J. Biol. Chem. **278:**37698–37704.

31. **Winterbottom, N., M. M. Tondravi, T. L. Harrington, F. G. Klier, B. M. Vertel, and P. F. Goetinck.** 1992. Cartilage matrix protein is a component of the collagen fibril of cartilage. Dev. Dyn. **193:**266–276.

32. **Wu, J. J., and D. R. Eyre.** 1998. Matrilin-3 forms disulfide-linked oligomers with matrilin-1 in bovine epiphyseal cartilage. J. Biol. Chem. **273:**17433–17438.